

Information System for Abandoned Arable Land Detection From Sentinel-2 Images

Karyna Akymenko^{1,†}, Kateryna Sergieieva^{1,*†}, Yurii Kavats² and Oleksandr Kovrov¹

¹ Dnipro University of Technology, av. Dmytra Yavornytskoho 19, 49005 Dnipro, Ukraine

² Ukrainian State University of Science and Technology, av. Nauky 4, 49005 Dnipro, Ukraine

Abstract

An information system for the automated detection of abandoned arable land, based on Sentinel-2 satellite images, is developed. The system provides monitoring of agricultural land, even in areas where ground surveys are challenging to conduct. Integrated with Google Earth Engine (GEE), the system classifies agricultural areas as cultivated or abandoned in near real time based on Normalized Difference Vegetation Index (NDVI) time series. It supports two modes of operation: local analysis of GeoTIFF files and cloud analysis using an interactive map. Its classification method compares the maximum NDVI values for the target and reference years, enabling the detection of the characteristics of the vegetation cover degradation of abandoned land. The results were experimentally validated for a sample of agricultural areas in the Dnipropetrovsk and Donetsk Oblasts. The proposed system can detect abandoned arable land with an accuracy of up to 92.5% (F₁-score: 0.898), even in areas of military conflict where ground observations are unavailable.

Keywords

information system, classification, NDVI, Sentinel-2, monitoring, abandoned arable land

1. Introduction

The problem of abandoned arable land has become particularly important in Ukraine in recent years due to the adverse environmental effects of the Russian invasion [1]. Even before the start of the Russo-Ukrainian War, numerous fields remained uncultivated. Still, military operations, the mining of territories, the disruption of logistical links, and general economic instability have significantly accelerated the degradation of agricultural land [2]. This has resulted in the loss of agricultural potential in many productive areas and the gradual overgrowth of the land by ruderal vegetation [3]. According to experts, approximately 2.4 million hectares of arable land have been abandoned since the start of the full-scale invasion of Ukraine, accounting for around 7.2% of the total area under cultivation [2]. The largest clusters of abandoned fields are concentrated in border regions affected by the conflict, particularly in eastern and southern Ukraine. The loss of cultivated land has complex negative consequences for food security, economic stability, and environmental conditions in agricultural regions [4].

2. Literature Review

Traditional ground-based monitoring is complicated and dangerous in wartime conditions, so satellite and GIS technologies are relevant, particularly Sentinel-2 data analysis. Ma et al. [5] demonstrated the effectiveness of remote sensing and GIS technologies for assessing the impact of

ICST-2025: Information Control Systems & Technologies, September 24-26, 2025, Odesa, Ukraine.

* Corresponding author.

† These authors contributed equally.

✉ akymenko.k.s@nmu.one (K. Akymenko); sergieieva.k.l@nmu.one (K. Sergieieva); yukavats@gmail.com (Yu. Kavats); kovrov.o.s@nmu.one (O. Kovrov)

ORCID: 0009-0008-2615-5015 (K. Akymenko); 0000-0001-7345-2209 (K. Sergieieva); 0000-0002-0180-5957 (Yu. Kavats); 0000-0003-3364-119X (O. Kovrov)



© 2025 Copyright for this paper by its authors. Use permitted under Creative Commons License Attribution 4.0 International (CC BY 4.0).

war on agricultural land in Ukraine. Nikulin et al. [6] proposed a method for detecting war-induced degradation of agricultural landscapes based on contrast edge changes in Sentinel-2 imagery. Hnatushenko et al. [7] developed a cloud-based geospatial information system for agricultural monitoring using Sentinel-2 data.

The Normalised Difference Vegetation Index (NDVI) has been successfully applied to detect abandoned agricultural land. Wei et al. [8] analysed spatial and temporal patterns of farmland abandonment using long-term satellite data. Morell-Monzó et al. [9] demonstrated the detection of abandoned citrus crops from Sentinel-2 time series. Wu et al. [10] monitored cropland abandonment in China using long-term NDVI dynamics.

In cultivated fields, the vegetation cycle is characterised by an increase in average NDVI values during the active growing season, reaching a maximum, and a subsequent decrease after harvest. However, on abandoned arable land, the seasonal dynamics of NDVI may differ. The amplitude of fluctuations varies depending on uncontrolled changes to the land's surface. At the same time, average NDVI values remain relatively high during the growing season due to the gradual development of wild vegetation, such as weeds, perennial grasses, shrubs, and trees. This indicates the formation of natural ecosystems with a predominance of spontaneous vegetation on such sites. A typical indicator of abandoned land in NDVI time series is a change in the cyclical growth curve and seasonal variability of vegetation indices [11, 12].

Traditional methods for analysing time series of vegetation indices focus on the maximum and minimum NDVI values during the growing season and the amplitude of seasonal fluctuations. This distinguishes cultivated and abandoned agricultural areas: the NDVI amplitude usually exceeds 0.6 for cultivated fields, while it is significantly lower for abandoned fields, often below 0.3 [2]. Changes are monitored by comparing NDVI maps from different years and analysing long-term observation series, which makes it possible to identify trends using linear or non-linear regression [13]. Analysing NDVI time series using maximum composite methods or comparing maximum index values for different years allows for the distinction between cultivated and abandoned fields [2].

In addition to NDVI, other spectral indices are used to identify abandoned arable land. These include the Enhanced Vegetation Index (EVI), which corrects for atmospheric and soil influences, and the Normalised Difference Moisture Index (NDMI), which reflects the moisture level in vegetation and soil cover, and indicates the cessation of irrigation and the beginning of degradation [9, 14]. Combining these indices enables the creation of composite maps of vegetation status; however, such approaches require high-quality data and may be less effective in complex terrain.

Analysing NDVI phenological profiles helps distinguish between cultivated crops at different development phases and abandoned areas dominated by spontaneous vegetation. Furthermore, digital elevation models (e.g., those based on LiDAR data) enable changes in vegetation height to be assessed, confirming the transformation of vegetation cover [12, 15].

Machine learning (ML) methods are increasingly being used due to the limitations of index methods, particularly with regard to their dependence on environmental conditions, incomplete time series data, and phenological variability [16]. The Random Forest (RF) method works effectively with a large set of spectral and auxiliary features, making no assumptions about their distribution and ensuring high classification accuracy [18]. The Support Vector Machine (SVM) method also enables binary classification with a limited training sample [19]. The most modern approaches combine image segmentation into objects with similar features, followed by ML classification. This allows objects' shape and texture to be considered, reducing errors associated with individual anomalous pixels [20]. However, existing algorithms have certain limitations: methods based on spectral indices can misinterpret natural changes as degradation, and ML models depend on local data and must be adapted to new regions. Difficulties arise in conflict zones due to the instability of agricultural cycles and situational land abandonment, which distorts time series. For this reason, the most effective approach is a combined one that analyses time series of spectral indices while considering the characteristics of the specific environment.

3. Aim and Objectives

This study aims to develop a methodology for identifying abandoned arable land based on the analysis of NDVI time series and classification results. The methodology is implemented and tested using a specially designed information system, which enables the distinction between cultivated and abandoned fields, essential for assessing the state of agroecosystems and for planning agricultural activities under conditions of environmental change, including those caused by armed conflict.

To achieve this aim, the following objectives were set:

1. Analyse the existing approaches to detecting abandoned agricultural land using remote sensing data.
2. Develop an NDVI-based classification method for distinguishing between cultivated and abandoned arable lands, including formulating classification rules and thresholds.
3. Design and implement an information system that automates data acquisition, NDVI calculation, time series analysis, and classification.
4. Validate the proposed methodology and the system's performance using reference data for selected arable areas in the Dnipropetrovsk and Donetsk Oblasts.
5. Assess the limitations of the proposed method and identify possible directions for further improvement.

4. Materials and Methods

4.1. Study area

The study examined agricultural areas in Ukraine, focusing primarily on the central region (Dnipropetrovsk Oblast), which was not directly affected by hostilities, and the eastern region (Donetsk Oblast), which was temporarily occupied at the time of the study and had suffered significant damage as a result of military operations. A sample of 53 test fields was analysed. The condition of the test fields in the Dnipropetrovsk Oblast was determined based on ground survey results, while the condition of the occupied and unoccupied territories was determined based on visual interpretation of Sentinel-2 satellite images.

The user interface of the developed system (Figure 1) enables users to define areas of analysis directly on the map and configure analysis parameters via the control panel. First, the range of years of study is set (e.g., 2020–2024), then the time limits of the growing season are selected (e.g., May to October). The system can check the availability of Sentinel-2 satellite images for a given territory and period, thus enabling the completeness of the input data to be assessed.

4.2. Satellite data

The study used Sentinel-2 L2A images with a maximum cloud cover of 15%. These images contain surface reflections (B0A) after atmospheric correction and were provided via the Copernicus Open Access Hub (<https://scihub.copernicus.eu/>) under an open access licence. The spectral bands B04 (665 nm), and B08 (842 nm) were used for the calculations. Access to the Sentinel-2 archive is available upon user request via the Google Earth Engine (GEE) platform using the API, with subsequent integration into the analysis toolkit [21].

The system is based on Sentinel-2 satellite data (COPERNICUS/S2_SR_HARMONISED collection) that have been pre-corrected for atmospheric effects using the Sen2Cor algorithm. The Scene Classification Layer (SCL) band, which contains data on the pixel-by-pixel classification of surface types, was used for preliminary image processing [22]. Based on this, a procedure was implemented to mask cloud cover and shadows to remove non-informative pixels from the input data [23].

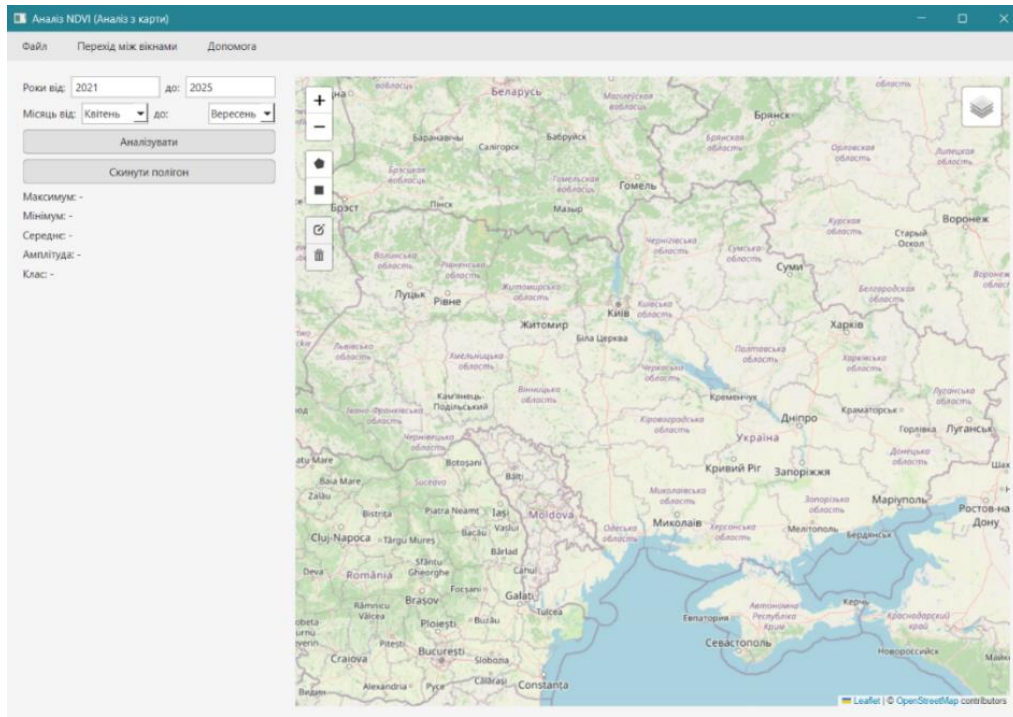


Figure 1: The interface of the mapping mode of the developed information system with visualization of the studied territory of Ukraine. Basemap: OSM Standard (EPSG:4326–WGS 84).

4.3. Abandoned arable land detection

4.3.1. Method for determining the arable land condition using NDVI time series

The Normalized Difference Vegetation Index (NDVI) is one of the earliest quantitative indicators of photosynthetically active biomass in vegetation cover [24]. Its values range from -1 to 1. Dense vegetation has NDVI values close to 1, while open ground has values around 0.2. NDVI is calculated as the difference between the reflectance values in the near infrared (NIR) and Red bands, divided by their sum:

$$NDVI = \frac{(\rho_{NIR} - \rho_{Red})}{(\rho_{NIR} + \rho_{Red})} = \frac{(\rho_{Band8} - \rho_{Band4})}{(\rho_{Band8} + \rho_{Band4})} \quad (1)$$

where ρ_{NIR}, ρ_{Red} – reflectance in NIR and Red spectral ranges, respectively,

$\rho_{Band8}, \rho_{Band4}$ – NIR (B08) and Red (B04) bands of sentinel-2 images.

A time series of NDVI values is formed for each field, which is pre-filtered by the specified years and months. The analysis is not performed if fewer than two years remain after filtering. The target year is determined from the available data – the last year in the set – and all previous years are considered as reference. The maximum NDVI value for the target year is calculated, as are the maximum values for each reference year [2]. The average of these maximums is compared with the maximum NDVI value for the target year. The difference between the maximums, or $\Delta NDVI$, is calculated as an indicator of changes (2).

$$\Delta NDVI = NDVI_{max}^{target} - \overline{NDVI_{max}^{reference}}, \quad (2)$$

where $NDVI_{max}^{target}$ – maximum NDVI value for the target season,

$\overline{NDVI_{max}^{reference}}$ – average value of NDVI maximums for reference seasons.

If this change is non-negative (i.e., NDVI has not decreased) and greater than the specified threshold T , the field is classified as cultivated. The field is considered abandoned if the change is negative and exceeds the predefined threshold absolute value (3). In the case where $\Delta NDVI = T$, the

field is considered abandoned, but additional clarification is desirable to determine the condition of the field by changing the data search criteria.

Classification rule:

If $\Delta\text{NDVI} > T \rightarrow$ **field is classified as cultivated arable land.**

If $\Delta\text{NDVI} \leq -T \rightarrow$ **field is classified as abandoned arable land,**

where T – threshold value for ΔNDVI .

The method used to classify agricultural areas as cultivated or abandoned is based on analysing changes to the NDVI index over time (Figure 2).

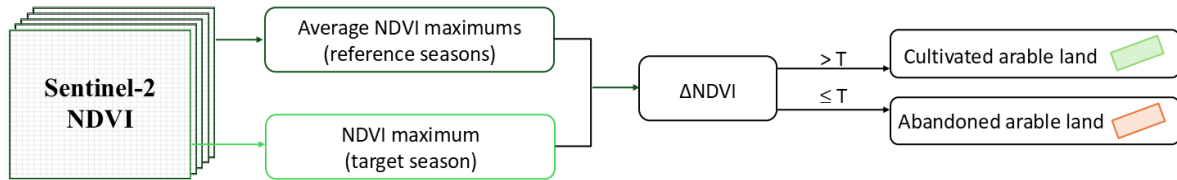


Figure 2: Method for determining the condition of arable land.

Generally, according to Figure 2, NDVI time series is formed by filtering Sentinel-2 L2A images by date, cloud cover ($\leq 15\%$, or any other value defined by user) and observation period limits (for example, January–December for the calendar year, or May–September for the growing season). Cloud and shadow pixels are masked using the Scene Classification Layer (SCL) and the NDVI is then calculated for each image. For each arable land polygon analyzed, the NDVI values are averaged over all pixels inside it to produce a chronological sequence. The maximum NDVI values are extracted for each observation period to apply formula (2) and the classification rule.

Data is processed in near real time. When working in cloud mode (GEE), calculations, including data visualization and the generation of an NDVI time series plot, take less than 10 seconds and depend on the field area.

4.3.2. Information system for abandoned arable land detection

An information system has been developed to automate the analysis of Sentinel-2 satellite data based on NDVI time series and to facilitate the classification of arable land as cultivated or abandoned. Its decision component uses a method that compares NDVI vegetation index maximums over multiple years and identifies deviations from typical seasonal dynamics. The Google Earth Engine (GEE) platform was used to access a global archive of satellite images and their pre-processing in the cloud. This allows users to select an area and configure analysis parameters. The system can request data independently, calculate the NDVI, analyse changes over the years, and make decisions about the condition of arable land.

The information system's architecture is modular (Figure 3), with function distribution between components. The system supports two operating modes: local analysis of NDVI time series using GeoTIFF data and remote analysis using GEE. The input data is pre-processed and normalised, after which NDVI is calculated, and a classification rule is used to determine fields as “cultivated” or “abandoned” based on temporal dynamics. The results are exported in tabular form and displayed to the user via an interactive map and plot.

The system consists of several interconnected components that provide a complete cycle of satellite data processing. Access to the Sentinel-2 image archive is supplied via the GEE API. Geospatial data processing uses the Rasterio 1.4, NumPy 2.2.0, Pandas 2.2.3, and Shapely 2.1.1 libraries. Visualisation is performed using Matplotlib 3.10.0 and Folium 0.19.7 [25]. The graphical interface, which is based on PySide6, enables users to interact with the system, set analysis polygons, and view the classification results in the form of interactive maps and plots. The classification method is based on analysing NDVI changes over time. It is deterministic, resistant to data gaps, and adaptable to research conditions.

The information system has two operating modes: local analysis of satellite GeoTIFF images and cloud analysis via integration with GEE. The main interface window is used to select the operating mode and serves as the entry point to the system. In local analysis mode, tools are available for downloading and processing data from local media. These include flexible configuration of study period parameters and output of key NDVI metrics. In cloud mode, users work with an interactive map on which they can draw polygons to define analysis areas and obtain classification results as pseudo-colour layers.

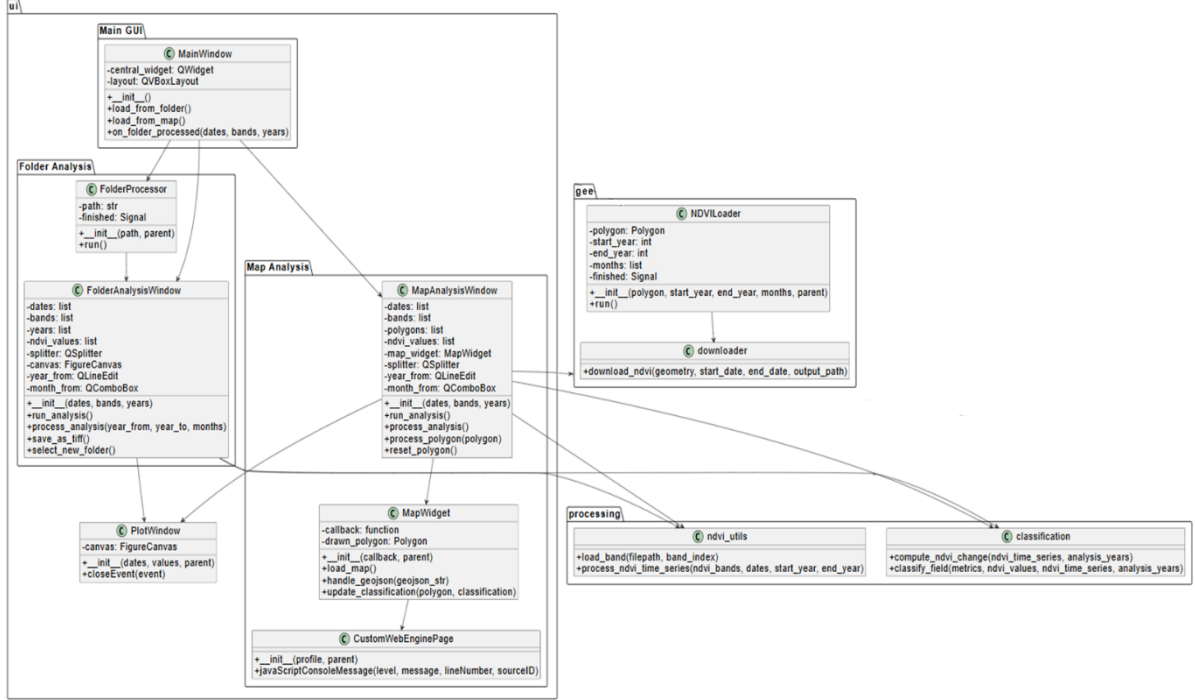


Figure 3: Class diagram of the developed information system.

The visualisation system enables viewing NDVI time series, and the programme menu allows managing operating modes, saving results, and accessing supporting information. The entire system focuses on intuitive interaction and supports cross-platform compatibility.

4.3.3. Accuracy assessment

This study used two approaches to assessing the accuracy of results: overall accuracy and F_1 -score [26].

Accuracy is the percentage of correctly classified fields relative to their total number.

A confusion matrix is generated to calculate the F_1 -score:

- True Positive (TP) – correctly identified as positive (e.g., “abandoned arable land”);
- True Negative (TN) – correctly identified as negative (e.g., “cultivated arable land”);
- False Positive (FP) – incorrectly identified as positive;
- False Negative (FN) – incorrectly identified as negative.

Precision is the proportion of objects belonging to a given class among all objects that the algorithm assigned to that class (the proportion of the “abandoned fields” class among all areas classified as “abandoned fields” by the classifier).

$$Precision = \frac{TP}{TP + FP} \quad (3)$$

Recall is the proportion of objects of a class found among all objects of that class (the probability that an object of the “abandoned fields” class will be classified as “abandoned fields”).

$$Recall = \frac{TP}{TP + FN} \quad (4)$$

The metric that combines information about the accuracy and completeness of a classifier is the F₁-score. The F₁-score is the harmonic mean between accuracy and completeness. It tends toward zero if accuracy or completeness tends toward zero.

$$F_1 = 2 \times \frac{Precision \times Recall}{Precision + Recall} = \frac{2TP}{2TP + FP + FN} \quad (5)$$

5. Results

To demonstrate the practical application of the developed information system, a complete cycle of analysis of arable land conditions was implemented in local and cloud modes. The procedure in local mode is described below as an example of a typical scenario for using the system.

After launching the main executable file in the Python environment, the system automatically initialises the necessary components, including checking the availability of external libraries, connecting to GEE, and loading configuration parameters. If initialisation is successful, the main window appears on the screen with two options: *'Run local analysis'* and *'Run cloud analysis'* from an interactive map.

To perform a local analysis, the user activates the *'Load from folder'* mode, which opens a dialogue box for selecting a directory containing satellite images in GeoTIFF format. After selecting the folder and setting the analysis parameters (e.g., the years and seasons of observation), the system filters the input data, calculates the basic statistical metrics of the NDVI index, and applies an algorithm to classify areas by condition.

The analysis results are displayed directly in the information panel. In particular, the user receives the following numerical characteristics:

- maximum NDVI value, which indicates maximum vegetation activity (e.g., 0.89);
- minimum NDVI, characteristic of the period of no vegetation in the field (e.g., 0.21);
- average NDVI, which summarizes the intensity of plant growth (e.g., 0.55);
- NDVI amplitude, which characterizes the strength of seasonal fluctuations (e.g., 0.68);
- field classification (e.g., “abandoned arable land”) determined by the results of an algorithmic comparison of NDVI over the years.

In addition to numerical metrics, the system automatically generates an NDVI time series plot for a given area. This plot opens in a separate window, enabling the user to visually assess seasonal NDVI dynamics, identify typical maxima and minima, and detect long-term trends indicating degradation or active land use.

Cloud mode runs similarly, processing data via the GEE platform based on an area defined by the user on an interactive map.

Consider the following example: using the developed information system to determine the condition of four fields near the Igren area in the eastern part of Dnipro city (Figure 4). Field 1 and Field 2, which are approximately 60 and 70 hectares, respectively, are cultivated using an annual crop rotation system. As of 1 June 2024, Field 1 had been sown with winter rapeseed and Field 2 with wheat. Field 3 has been abandoned for over 20 years and is overgrown with shrubbery. Field 4 had been abandoned for three years and, at the time of the 24 May 2025 survey, was covered in the dry remains of last year's vegetation.

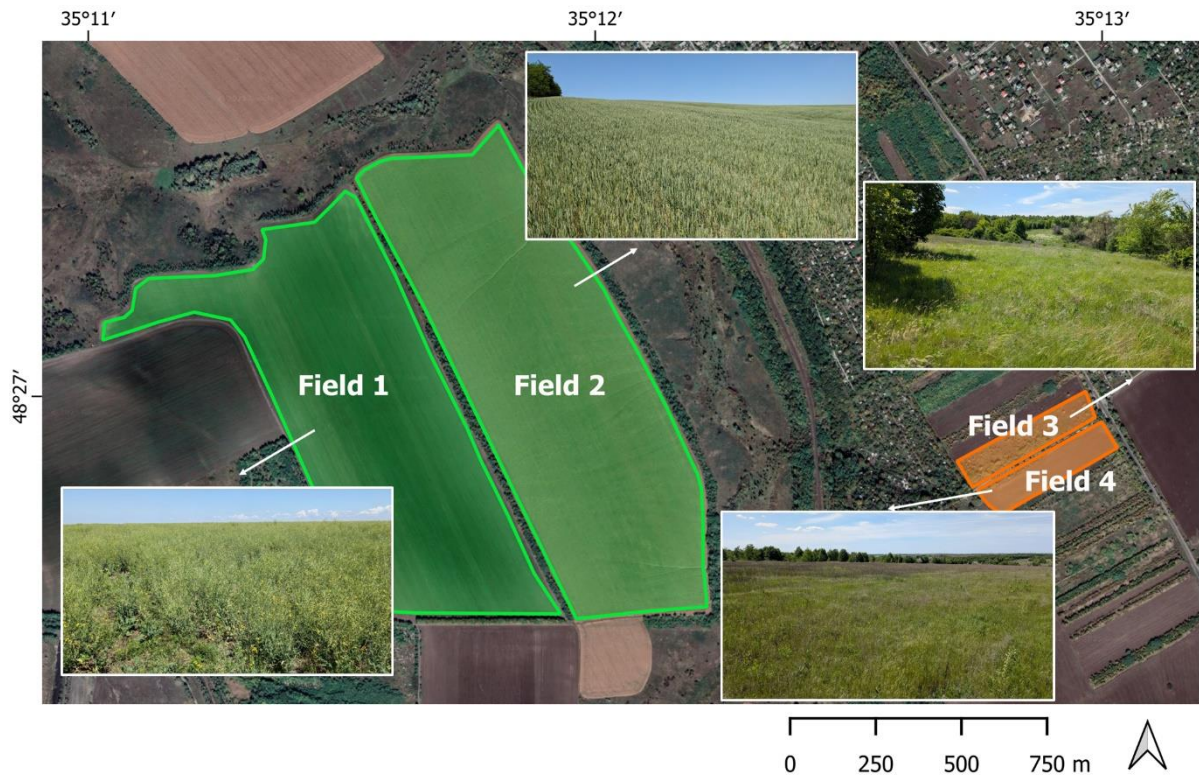


Figure 4: Location of cultivated and abandoned fields in the Dnipropetrovsk Oblast. Basemap: Google Satellite.

Figure 5 shows Sentinel-2 RGB images of the study fields acquired on 9 July 2024 and 29 July 2025. In 2024, Field 1 and Field 2 were planted with winter crops. By the time the images were taken, the harvest had already been completed (Figure 5a). Field 1 was also planted with winter crops in 2025, and the harvest had been completed by 29 July 2025 (Figure 5b). Field 2 was not sown in the 2025 season, and after spring cultivation, it was left as temporary fallow land. Field 3 and Field 4 have been abandoned for several years, and their appearance in summer remains unchanged each year (Figure 5). These abandoned areas are evenly covered with weeds and exhibit a typical growth and wilting cycle, with no pronounced signs of technological impact such as cultivation, harvesting, or ploughing.

Figure 6 shows the time series of maximum NDVI values for each date for two cultivated fields (Fields 1 and 2, Figures 6a and 6b) and two uncultivated fields (Fields 3 and 4, Figures 6c and 6d), as shown in Figure 4. The long-term average maximum NDVI values are 0.964 for Field 1, 0.956 for Field 2, 0.949 for Field 3, and 0.937 for Field 4. While all the fields demonstrate maximum NDVI values exceeding 0.93, the dynamics of the vegetation index vary depending on land use.

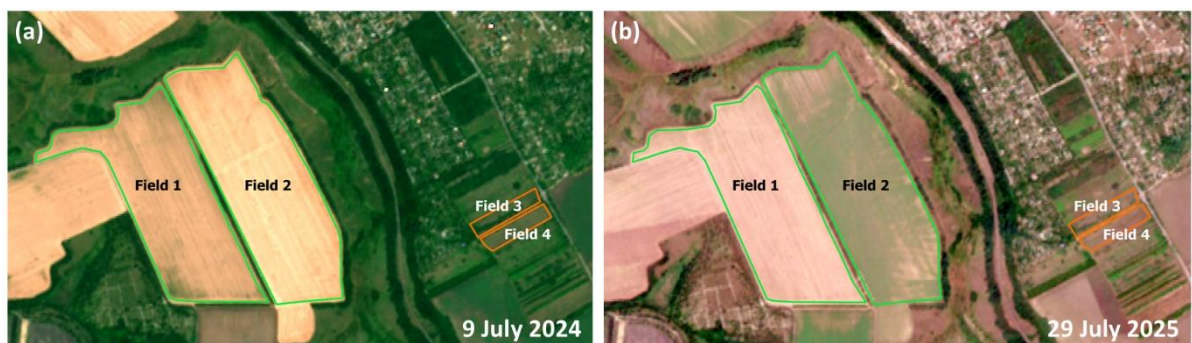


Figure 5: Sentinel-2 RGB-images of cultivated and abandoned fields: (a) 9 July 2024; (b) 29 July 2025.

Stable NDVI mode values are observed throughout the observation period for cultivated fields, indicating active agricultural production. Uncultivated fields also demonstrate high mode values; however, the overall shape of the time series differs, with clear seasonal intermodal minima visible. These local decreases in NDVI indicate natural seasonal changes in vegetation cover characteristic of degraded or abandoned land and the presence of dry residues of last year's plants in the field in late spring.

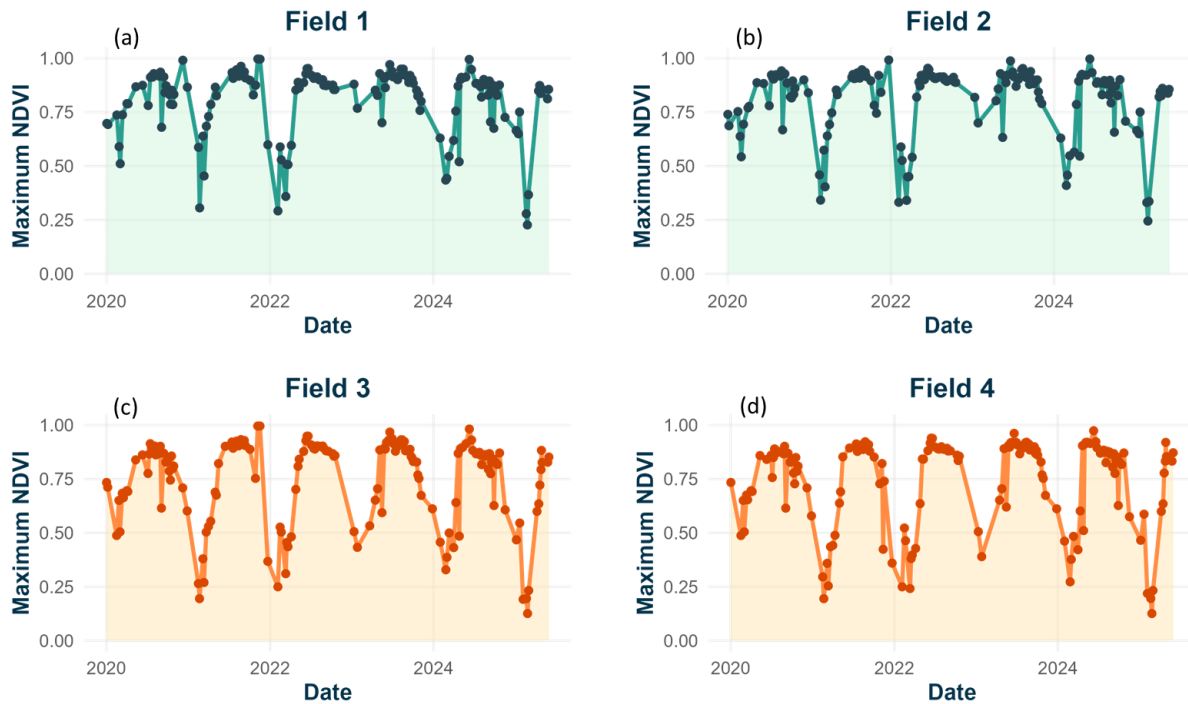


Figure 6: Time series of maximum NDVI for cultivated (a, b) and abandoned (c, d) arable land: (a) Field 1; (b) Field 2; (c) Field 3; (d) Field 4.

In comparison, such intermodal minima are less pronounced in cultivated fields. This may be due to the cultivation of winter crops, which produce relatively high NDVI values during the cold season and thus smooth out seasonal fluctuations in NDVI.

For quantitative comparison, the average minimum NDVI values for all years of observation were calculated. These are: 0.412 for Field 1, 0.418 for Field 2, 0.304 for Field 3, and 0.286 for Field 4. While the values are similar, the dynamics – specifically, the presence or absence of seasonal declines in NDVI – are a key indicator of land use patterns. The stability of mode values alongside a change in the inter-seasonal structure of NDVI is a characteristic feature of abandoned land. This pattern is not observed for cultivated fields due to the peculiarities of crop rotation.

An analysis of the difference (ΔNDVI) between the long-term average maximum NDVI and the current year's maximum showed that, for uncultivated fields, this difference generally does not exceed the threshold value of 0.07. This threshold value was used as a classification criterion within the developed system. According to the validation results, this value ensured an accuracy level of 92.5% for classifying field condition (cultivated/abandoned) in Ukraine, with an F_1 -score for abandoned arable land: 0.898, cultivated: 0.912. The reported accuracy refers specifically to the tested sample of fields and should not be directly generalized to the entire territory of the Dnipropetrovsk and Donetsk Oblasts.

Field conditions in the Dnipropetrovsk Oblast were determined using ground surveys. In the Donetsk Oblast, where access was restricted due to hostilities, field conditions were determined via expert visual interpretation of multi-temporal Sentinel-2 imagery (10 m resolution) for multiple years. While such data provides valuable insights into inaccessible regions, it is inherently less reliable than ground truth measurements and is considered accordingly in the accuracy assessment.

6. Discussion

The developed information system for detecting abandoned arable land confirms the feasibility of combining geoinformatics and satellite monitoring methods [27, 28]. The system is based on analysing NDVI time series obtained from Sentinel-2 images with high spatial and temporal resolution, which are available via the GEE platform. This approach enables land conditions to be assessed without field surveys, which is particularly relevant when access to territories is limited.

Abandoned arable lands are identified by comparing maximum NDVI values in reference and target periods, enabling changes in vegetation activity associated with cessation of land use to be detected. Using the proposed threshold classification method reduces the impact of seasonal anomalies, weather factors, and war-related damage, and simplifies the interpretation of results. Forming a temporal NDVI map for each field allows changes in land use intensity to be visualised and the extent of agricultural landscape degradation to be assessed.

The system has a dual architecture that supports two modes: local analysis of GeoTIFF files and cloud-based processing of GEE data. This provides flexibility and adaptability to different conditions, from working with local archives to interactive, real-time analytics [29]. Users can outline an area directly on the map, set analysis parameters, and visualise the results as pseudo-colour layers and a time series plot. A statistical analysis module has also been implemented, which outputs key metrics such as maximum, minimum, average values, and NDVI amplitude. It classifies the field according to the proposed criteria.

The data preprocessing stage includes cloud masking based on the Scene Classification Layer, calculating the Normalised Difference Vegetation Index (NDVI), and aggregating by vegetation periods. This improves the accuracy of the estimates. According to the validation results, the accuracy of classifying abandoned fields was 92.5% (F_1 -score for abandoned arable lands: 0.898, cultivated: 0.912) in typical Ukrainian agricultural landscapes. The accuracy of the results obtained is comparable to that of other researchers. For example, Du et al. [26] provided the results of agricultural land abandonment and retirement mapping in Northern China using a trajectory-based change detection approach with 87–92% overall accuracy and F_1 -score for abandoned lands: 0.74, retired: 0.83. The results of agricultural land mapping by He et al. [11] showed that rain-fed abandoned agricultural land had lower F_1 -score values (from 0.759 to 0.8) compared to irrigated agricultural land (from 0.836 to 0.879) at an overall accuracy of about 90%. Xie et al. [30] developed a USA nationwide, 30 m resolution map of croplands abandoned from 1986 to 2018 using satellite images at up to 91% accuracy.

It should be noted that the experimental validation was based on a relatively small dataset of 53 fields, which limits the ability to generalize the obtained accuracy metrics to larger territories. Furthermore, the reference data were obtained via expert visual interpretation of satellite imagery rather than direct ground observations for areas in the Donetsk Oblast under temporary occupation. This factor may introduce additional uncertainty into the validation results. Future work will address these limitations by expanding the sample size and incorporating more comprehensive ground truth datasets from multiple regions of Ukraine.

Additional limitations of the proposed method relate to situations where a field remains unsown due to non-war-related factors, such as drought or economic constraints, or where cultivation occurs but vegetation fails to develop due to severe soil degradation. In such cases, the NDVI time series may resemble the pattern of abandoned land, leading to false positives. Similarly, temporary land abandonment or shifts in cropping schedules can distort the seasonal NDVI profile. These situations are particularly relevant in combat zones, where infrastructure damage, soil contamination, and irregular management practices can disrupt regular phenological cycles. To address these cases, future system iterations will incorporate additional data sources such as meteorological observations, Synthetic Aperture Radar (SAR) imagery, and optional expert review for ambiguous results.

It should be noted that, in its current implementation, the system uses only NDVI as the primary indicator for classification. Other indices, such as EVI and NDMI, have not yet been integrated into the operational workflow. This limitation may reduce robustness under conditions of high cloud

cover, seasonal anomalies, or phenological variability. The planned integration of these additional data sources will enable the system to operate more reliably in challenging weather conditions, improve classification accuracy in heterogeneous landscapes, and extend the analysis to periods or regions where optical data are insufficient. Further proposed developments to the system include integration with additional data sources, particularly Sentinel-1 SAR images, to enable all-weather monitoring [31, 32]. The range of vegetation indices can also be expanded for better crop differentiation, and machine learning algorithms can be developed for automatic land cover classification. A mobile version can also be implemented for use in the field [33, 34]. Furthermore, creating an API will enable integration with other GIS solutions and connection to databases for the long-term storage of results [35]. The developed system demonstrates the practical value of integrating satellite data, mathematical processing methods, and software technologies for decision support tools in land resource management. System implementation will improve agricultural land use and food security management.

7. Conclusions

The information system is developed to provide automated classification of arable land as cultivated or abandoned, based on an analysis of the NDVI time series from Sentinel-2 images, with an accuracy of up to 92.5% and F_1 -score 0.898 for abandoned arable land. Integration with Google Earth Engine enables processing large volumes of satellite data in the cloud for near-real-time monitoring. The system is based on a proposed method of classifying agricultural field conditions that compares maximum NDVI values for different years. This allows land degradation to be detected even without ground surveys under war conditions. Further system development includes integrating Sentinel-1 data for all-weather monitoring and expanding the range of vegetation indices to improve differentiation of land use types. Developing machine learning algorithms and a mobile version will also enhance classification accuracy and facilitate rapid on-site analysis.

Acknowledgements

This study was funded by the Ministry of Education and Science of Ukraine under the research work “The development of environmentally safe technologies for the restoration of man-made degraded territories in the conditions of post-war reconstruction” (0124U000357).

The authors would like to thank the European Commission, the European Space Agency, and the Copernicus Program for providing Sentinel data.

Declaration on Generative AI

The authors have not employed any Generative AI tools.

References

- [1] T. He, M. Zhang, W. Xiao, G. Zhai, Y. Wang, A. Guo, C. Wu, Quantitative analysis of abandonment and grain production loss under armed conflict in Ukraine, *J. Clean. Prod.* 412 (2023) 137367. doi:10.1016/j.jclepro.2023.137367.
- [2] K. Dai, C. Cheng, S. Kan, Y. Li, K. Liu, X. Wu, Impact of arable land abandonment on crop production losses in Ukraine during the armed conflict, *Remote Sensing* 16 (2024) 4207. doi:10.3390/rs16224207.
- [3] S. Nikulin, K. Sergieieva, Assessing degradation of war-affected anthropogenic landscape using Sentinel-2 images, *International Journal of Remote Sensing* 46 (2025) 5732–5772. doi:10.1080/01431161.2025.2526001.
- [4] S. Zhang, Y. Zhang, X. Zhang, C. Miao, S. Liu, J. Liu, Revealing the distribution and change of abandoned cropland in Ukraine based on dual period change detection method, *Scientific Reports* 15 (2025) 5765. doi:10.1038/s41598-025-89556-2.

- [5] Y. Ma, D. Lyu, K. Sun, S. Li, B. Zhu, R. Zhao, M. Zheng, K. Song, Spatiotemporal analysis and war impact assessment of agricultural land in Ukraine using RS and GIS technology, *Land* 11 (2022) 1810. doi:10.3390/land11101810.
- [6] S. L. Nikulin, K. L. Sergieieva, O. V. Korobko, Assessment of war-damaged agricultural landscape degradation in Ukraine using satellite-based contrast edge changes, in: *Proceedings of the XVIII International Scientific Conference "Monitoring of Geological Processes and Ecological Condition of the Environment"*, EAGE, Kyiv, Ukraine, 2025, pp. 1–5. doi:10.3997/2214-4609.2025510117.
- [7] V. V. Hnatushenko, K. Y. Sierikova, I. Y. Sierikov, Development of a cloud-based web geospatial information system for agricultural monitoring using Sentinel-2 data, in: *Proceedings of the IEEE 13th International Scientific and Technical Conference on Computer Sciences and Information Technologies (CSIT)*, IEEE, Lviv, Ukraine, 2018, pp. 270–273. doi:10.1109/STC-CSIT.2018.8526717.
- [8] Z. Wei, X. Gu, Q. Sun, X. Hu, Y. Gao, Analysis of the spatial and temporal pattern of changes in abandoned farmland based on long time series of remote sensing data, *Remote Sensing* 13 (2021) 2549. doi:10.3390/rs13132549.
- [9] S. Morell-Monzó, M.T. Sebastiá-Frasquet, J. Estornell, E. Moltó, Detecting abandoned citrus crops using Sentinel-2 time series: A case study in the Comunitat Valenciana region (Spain), *ISPRS Journal of Photogrammetry and Remote Sensing* 201 (2023) 54–66. doi:10.1016/j.isprsjprs.2023.05.003.
- [10] J. Wu, S. Jin, G. Zhu, J. Guo, Monitoring of cropland abandonment based on long time series remote sensing data: A case study of Fujian Province, China, *Agronomy* 13 (2023) 1585. doi:10.3390/agronomy13061585.
- [11] S. He, H. Shao, W. Xian, Z. Yin, M. You, J. Zhong, J. Qi, Monitoring cropland abandonment in hilly areas with Sentinel-1 and Sentinel-2 time series, *Remote Sensing* 14 (2022) 3806. doi:10.3390/rs14153806.
- [12] T. Liu, L. Yu, X. Liu, D. Peng, X. Chen, Z. Du, Q. Zhao, A global review of monitoring cropland abandonment using remote sensing: temporal–spatial patterns, causes, ecological effects, and future prospects, *Journal of Remote Sensing* 5 (2025) 0584. doi:10.34133/remotesensing.0584.
- [13] E. Portalés-Julià, M. Campos-Taberner, F. J. García-Haro, M. A. Gilabert, Assessing the Sentinel-2 capabilities to identify abandoned crops using deep learning, *Agronomy* 11 (2021) 654. doi:10.3390/agronomy11040654.
- [14] K. Hazaymeh, W. Sahwan, S. Al Shogoor, B. Schütt, A remote sensing-based analysis of the impact of Syrian crisis on agricultural land abandonment in Yarmouk River Basin, *Sensors* 22 (2022) 3931. doi:10.3390/s22103931.
- [15] J. Janus, P. Bozek, Aerial laser scanning reveals the dynamics of cropland abandonment in Poland, *Journal of Land Use Science* 14 (2019) 378–396. doi:10.1080/1747423X.2019.1709226.
- [16] X. Wu, N. Zhao, Y. Wang, Y. Ye, W. Wang, T. Yue, Y. Liu, The potential role of abandoned cropland for food security in China, *Resources, Conservation and Recycling* 212 (2025) 108004. doi:10.1016/j.resconrec.2024.108004.
- [17] H. Yoon, S. Kim, Detecting abandoned farmland using harmonic analysis and machine learning, *ISPRS Journal of Photogrammetry and Remote Sensing* 166 (2020) 201–212. doi:10.1016/j.isprsjprs.2020.05.021.
- [18] W. Meijninger, B. Elbersen, M. van Eupen, S. Mantel, P. Ciria, A. Parenti, A. Monti, Identification of early abandonment in cropland through radar-based coherence data and application of a Random-Forest model, *GCB Bioenergy* 14 (2022) 735–755. doi:10.1111/gcbb.12939.
- [19] F. Löw, E. Fliemann, I. Abdullaev, C. Conrad, J. P. Lamers, Mapping abandoned agricultural land in Kyzyl-Orda, Kazakhstan using satellite remote sensing, *Applied Geography* 62 (2015) 377–390. doi:10.1016/j.apgeog.2015.05.009.
- [20] D. Wuyun, L. Sun, Z. Chen, L.G.T. Crusiol, J. Dong, N. Wu, H. Zhao, Temporal segmentation method for 30-meter long-term mapping of abandoned and reclaimed croplands in Inner

- Mongolia, China, *International Journal of Applied Earth Observation and Geoinformation* 136 (2025) 104399. doi:10.1016/j.jag.2025.104399.
- [21] S. Xu, W. Xiao, C. Yu, H. Chen, Y. Tan, Mapping cropland abandonment in mountainous areas in China using the Google Earth Engine platform, *Remote Sensing* 15 (2023) 1145. doi:10.3390/rs15041145.
- [22] C. Sanchez, F. Mena, M. Charfuelan, M. Nuske, A. Dengel, Assessment of Sentinel-2 spatial and temporal coverage based on the scene classification layer, in: *Proceedings of the IGARSS 2024 - 2024 IEEE International Geoscience and Remote Sensing Symposium*, IEEE, Athens, Greece, 2024, pp. 4099–4103. doi:10.1109/IGARSS53475.2024.10642213.
- [23] Y. I. Shedlovska, V. V. Hnatushenko, Shadow removal algorithm with shadow area border processing, in: *Proceedings of the II International Young Scientists Forum on Applied Physics and Engineering (YSF)*, IEEE, Kharkiv, Ukraine, 2016, pp. 164–167. doi:10.1109/YSF.2016.7753827.
- [24] J. W. Rouse, R. H. Haas, J. A. Schell, D. W. Deering, Monitoring vegetation systems in the Great Plains with ERTS, in: *Proceedings of the 3rd ERTS Symposium*, NASA SP-351 I, 1973, pp. 309–317.
- [25] M. Shreenithi, M. Sujithra, B. Senthilkumar, D. Shanmugapriyaa, T. Rizanuma, Spatial data visualization with Python: techniques, tools, and real, in: M. G. Galety, A. K. Natarajan, T. F. Gedefa, T. D. Lemma (Eds.), *Geospatial Application Development Using Python Programming*, 2024, pp. 123–162. doi:10.4018/979-8-3693-1754-9.ch005.
- [26] Z. Du, J. Yang, C. Ou, T. Zhang, Agricultural land abandonment and retirement mapping in the northern China crop-pasture band using temporal consistency check and trajectory-based change detection approach, *IEEE Transactions on Geoscience and Remote Sensing* 60 (2021) 1–12. doi:10.1109/TGRS.2021.3121816.
- [27] J. S. Visockiene, E. Tumeliene, V. Maliene, Analysis and identification of abandoned agricultural land using remote sensing methodology, *Land Use Policy* 82 (2019) 709–715. doi:10.1016/j.landusepol.2019.01.013.
- [28] M. E. Kabadayı, P. Ettehadi Osgouei, E. Sertel, Agricultural land abandonment in Bulgaria: a long-term remote sensing perspective, 1950–1980, *Land* 11 (2022) 1855. doi:10.3390/land11101855.
- [29] V. Hnatushenko, V. Shuleshko, T. Bulana, B. Molodets, Information system to enhance agricultural production efficiency based on sustainable development principles, in: *Proceedings of the AdvAIT-2024: 1st International Workshop on Advanced Applied Information Technologies*, CEUR, Khmelnytskyi, Ukraine – Zilina, Slovakia, 2024. <https://ceur-ws.org/Vol-3899/paper2.pdf>.
- [30] Y. Xie, S. A. Spawn-Lee, V. C. Radeloff, H. Yin, G. P. Robertson, T. J. Lark, Cropland abandonment between 1986 and 2018 across the United States: spatiotemporal patterns and current land uses, *Environmental Research Letters* 19(4) (2024) 044009. doi:10.1088/1748-9326/ad2d12.
- [31] T. Bucha, J. Papčo, I. Sačkov, J. Pajčík, M. Sedliak, I. Barka, J. Feranec, Woody above-ground biomass estimation on abandoned agriculture land using Sentinel-1 and Sentinel-2 data, *Remote Sensing* 13 (2021) 2488. doi:10.3390/rs13132488.
- [32] B. Qiu, D. Lin, C. Chen, P. Yang, Z. Tang, Z. Jin, Z. Chen, From cropland to cropped field: a robust algorithm for national-scale mapping by fusing time series of Sentinel-1 and Sentinel-2, *International Journal of Applied Earth Observation and Geoinformation* 113 (2022) 103006. doi:10.1016/j.jag.2022.103006.
- [33] W. Song, Mapping cropland abandonment in mountainous areas using an annual land-use trajectory approach, *Sustainability* 11 (2019) 5951. doi:10.3390/su11215951.
- [34] K. Zhou, X. Zheng, How does the growth of digital technology influence farmland abandonment? Evidence from rural China, *Sustainability* 17 (2025) 2227. doi:10.3390/su17052227.
- [35] Z. Yu, C. Lu, Historical cropland expansion and abandonment in the continental US during 1850 to 2016, *Global Ecology and Biogeography* 27 (2018) 322–333. doi:10.1111/geb.12697.